https://doi.org/10.5194/egusphere-2026-4407
Preprint. Discussion started: 12 August 2026

Increasing model parsimony without loss of process fidelity: a simplified LASCAM rainfall-runoff model

Ziqi Zhang[1], Keirnan Fowler[1], Margot Turner[2], Joel Hall[2]

[1]Department of Infrastructure Engineering, University of Melbourne, Melbourne, 3010, Victoria, Australia
[2]Department of Water and Environmental Regulation, Joondalup, 6027, Western Australia, Australia

Correspondence to: Ziqi Zhang (ziqi.zhang20@unimelb.edu.au)

Abstract. Rainfall-runoff models are widely used to support water resource planning, yet many struggle under prolonged drought. During these periods, cumulative water deficits can strongly affect streamflow response by altering vegetation water use and contributing to multi-annual storage dynamics. The Large Scale Catchment Model (LASCAM) is well suited to representing these processes through its deep groundwater store and flux structure, but its large number of calibrated parameters increases computational cost and limits practical application. This study developed a simplified version of LASCAM by reducing the number of free parameters while retaining the structural features of the original model. Using the latest version of LASCAM (LASCAM22) as the starting point, we applied a staged simplification procedure that combined sensitivity analysis, parameter default-value testing, and stepwise parameter-fixing calibration. The reduced configuration was then compared with GR4J, Sacramento, and LASCAM22 in split-sample testing. Several low-sensitivity parameters were fixed with limited loss of performance, while the stepwise parameter-fixing calibration supported the 15-parameter configuration (LASCAM15) as the best compromise between dimensionality reduction and performance retention. In the split-sample test, LASCAM15 achieved stronger validation performance than LASCAM22 and outperformed GR4J and Sacramento during both calibration and validation. The resulting model is more parsimonious (i.e., fewer calibrated parameters), is more computationally efficient to calibrate, and provides more robust simulations for catchment modelling applications.

1 Introduction

Rainfall-runoff models are widely used to support water resource planning, but many struggle to reproduce catchment response during prolonged droughts (Fowler et al., 2020; Saft et al., 2016; Vaze et al., 2010). This is a major challenge for future planning under climate change, as droughts are expected to become more frequent and severe in many regions (Cook et al., 2018; Lehner et al., 2017). Conceptual rainfall-runoff models are particularly useful in this context because they are sufficiently parsimonious to be integrated into decision making and/or support exploration of uncertainty in future outcomes.
Recent studies have highlighted the importance of vegetation dynamics and groundwater memory in shaping catchment response to prolonged drought in some regions (e.g., Alvarez-Garreton et al., 2021; Avanzi et al., 2020; Campion et al.,

https://doi.org/10.5194/egusphere-2026-4407
Preprint. Discussion started: 12 August 2026

2026; Fowler et al., 2022; Hughes et al., 2012; Massari et al., 2022; Peterson et al., 2021). These findings emphasize the value of models that can better represent vegetation water use dynamics and longer-term storage dynamics when investigating drought response. In this regard, the Large Scale Catchment Model (LASCAM) is a particularly relevant conceptual rainfall-runoff model: Burns et al. (2025) showed that its actual evapotranspiration (AET) formulation was the most accurate among the equations evaluated against flux tower observations compared to 46 other conceptual rainfall runoff models. Meanwhile, Zhang et al. (2026) identified LASCAM as one of only six models capable of capturing multi-annual storage dynamics. Together, these findings suggest that LASCAM is well suited for investigating catchment response under prolonged dry conditions, compared to other conceptual rainfall-runoff models.

LASCAM was developed in Western Australia to simulate the long-term effects of land-use and climate change on streamflow and water quality (Sivapalan et al., 1996a, b, c, 2002; Viney and Sivapalan, 1999; Viney et al., 2000). Originally derived from catchment water and salt balance studies, it was later extended from small forested catchments to larger systems through a subcatchment-based structure (e.g., Viney and Sivapalan, 2001; Zammit et al., 2005). In this study, we focus on the water balance component of LASCAM, implemented as a lumped model, which represents catchment hydrology using a set of conceptual hillslope stores and fluxes. This includes three main stores: the A store, representing the near-stream perching layer and riparian zone; the B store, representing the deeper groundwater system; and the F store, representing an unsaturated infiltration store (Ye et al., 1997). Through these stores, incoming rainfall is partitioned into surface and subsurface pathways, including infiltration, inter-store recharge, evaporation losses, saturation-excess and infiltration-excess runoff, and discharge to the stream (Sivapalan et al., 1996a). More recently, LASCAM has been adapted for implementation in eWater SOURCE, Australia's hydrological modelling platform (Welsh et al., 2013), highlighting its continued relevance for applied catchment modelling in Australia.

However, LASCAM remains relatively complex, with current versions ranging from 22 to 28 parameters requiring calibration, including parameters controlling throughfall, surface and subsurface saturation and infiltration, store-specific discharge and evaporation, and upslope perching processes (e.g., Knoben et al., 2019). This level of complexity can hinder practical application by increasing calibration effort and reducing model interpretability. Also, the information content of commonly available hydrological observations is often insufficient to constrain a large number of parameters (e.g., Jakeman and Hornberger, 1993). For example, in a recent comparison of conceptual rainfall-runoff models using the MARRMoT framework (Knoben et al., 2019; Trotter et al., 2021), LASCAM showed strong performance in realistically transitioning between decadal wetting and drier periods, but its computational cost was sufficiently high that not all planned tested could even be complected (Campion et al., 2024). In such cases, additional complexity does not necessarily improve model performance and may instead increase uncertainty in simulated internal states and fluxes (Merz et al., 2022; Perrin et al., 2001), consistent with the problem of equifinality in hydrological modelling (Beven, 2006; Bouaziz et al., 2021). As a result, parameter values in LASCAM may be difficult to identify uniquely, model behaviour may be harder to interpret, and predictive confidence may be reduced when the model is applied beyond the calibration period or under changing climatic conditions.

https://doi.org/10.5194/egusphere-2026-4407
Preprint. Discussion started: 12 August 2026

To address this challenge, this study develops a simplified version of the LASCAM water balance model, with the aim of reducing calibration burden while retaining the key structural and process-based features that underpin the original model's value. The simplified model (which we call LASCAM15) is presented as Python code while also implemented as a plugin within the national modelling framework mentioned above (eWater SOURCE), enabling its direct use in practical catchment modelling applications. This outcome supports water planning by enabling faster scenario testing, clearer comparison of drought-management options, and easier integration of catchment response modelling into existing planning workflows. In doing so, the study seeks to provide a more parsimonious and operationally accessible framework for investigating catchment response under prolonged drought.

2 Study area and data

This study focused on catchments in South-West Western Australia (SWWA), a region that has experienced substantial rainfall and streamflow decline, particularly since the late 1990s. LASCAM was originally developed for application in this region, making SWWA a suitable study area for testing whether the model could be simplified while retaining its existing hydrological structure. The analysis used two levels of catchment assessment: a focal set of seven primary catchments for detailed development of the simplification procedure, and a wider regional sample of 76 SWWA catchments for broader testing and final model selection. The locations of the catchments used in the study are shown in Fig. 1.

The seven primary catchments were Gingin Brook (617058), Wooroloo Brook (616001), Serpentine River (614030), Harvey River (613002), Margaret River (610001), Scott River (609002), and Record Brook (608007). These catchments were selected to broadly cover the range of hydroclimatic and hydrological conditions across SWWA, and each of them have long streamflow records spanning 1990 to 2026, high-quality flow gauging structures, and limited direct human impacts from land-use change, in-stream pumping, dams, or diversions over the period of record. The primary catchments range from catchments on sandy coastal plains with low relief, primarily cleared land cover, and permanent groundwater inputs, to ephemeral catchments on granite-based escarpments with fully forested land cover.

The wider regional sample was used to evaluate the simplified configurations across a broader range of SWWA catchments. These catchments covered much of the regional modelling domain, spanning coastal-plain, plateau, and upland settings with substantial variation in topography, geology, climate, and runoff response. The sample was selected to include catchments of practical interest for water resource planning, while also providing broad regional coverage for evaluating model robustness. Catchments with significant extractions or direct human impacts were avoided where possible, although some impacted catchments were retained where they were considered important for regional assessment.

Daily climate inputs for the selected catchments were obtained from the SILO climate database (https://www.longpaddock.qld.gov.au/silo/point-data). Daily streamflow data were obtained mainly from the CAMELS-AUS v2 database (Fowler et al., 2025), supplemented by records from the DWER Water Information Reporting database (http://wir.water.wa.gov.au) for stations not included in CAMELS-AUS v2.

https://doi.org/10.5194/egusphere-2026-4407
Preprint. Discussion started: 12 August 2026

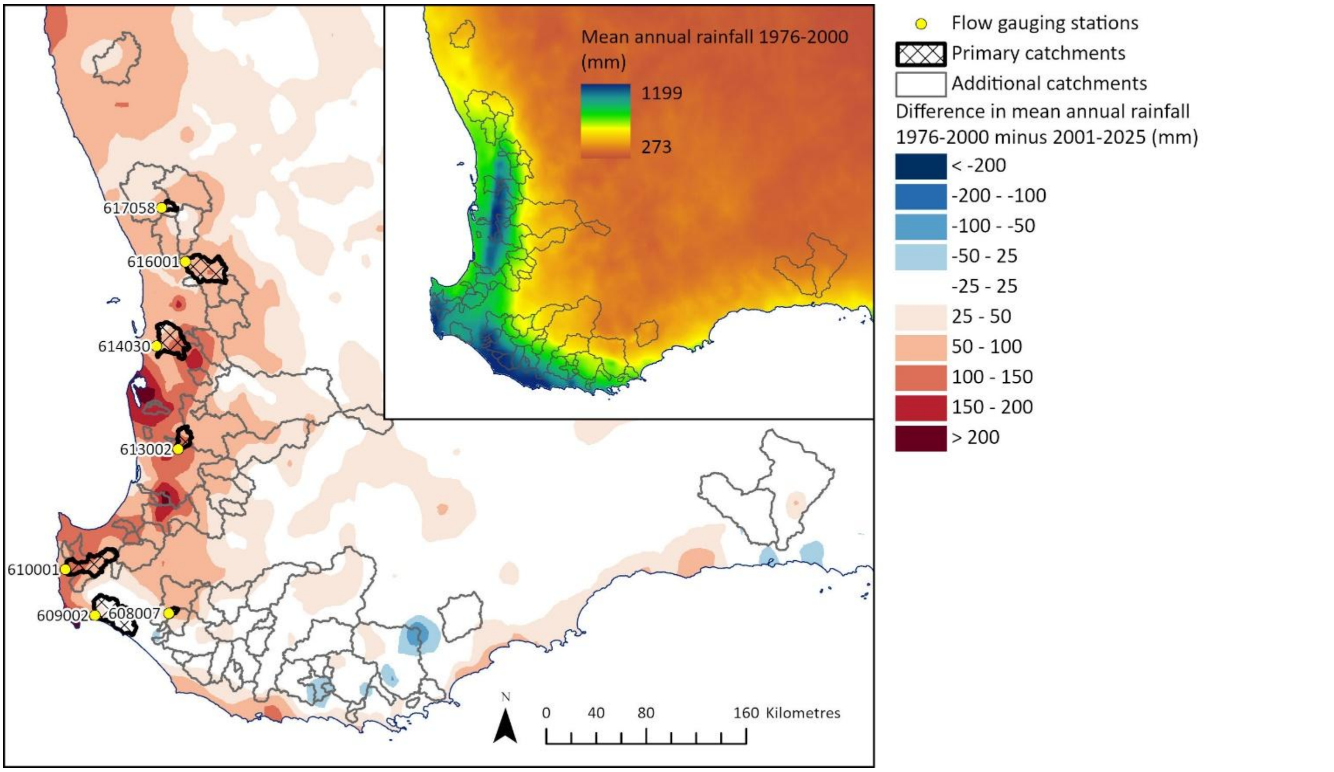

Figure 1. Locations of the study catchments in South-West Western Australia. The seven primary catchments used to inform the detailed model simplification procedure are shown with thicker black boundaries and yellow flow-gauging stations, while the wider regional sample used for broader testing are shown with thinner grey boundaries. Background shading shows the difference in mean annual rainfall between 1976-2000 and 2001-2025, with positive values indicating lower rainfall in the later period.

3 LASCAM structure

Several versions of LASCAM have been developed, differing mainly in the processes and endpoints simulated (e.g., some versions simulate salinity) and number of calibrated parameters. In this study, we use the most recent version of the model as the starting point for model simplification (Campion et al., 2024). This version contains 22 calibrated parameters and is hereafter referred to as LASCAM22 for clarity.

LASCAM22 is a simplified form of the eWater Source version of LASCAM, which contains 28 calibrated parameters (hereafter referred to as LASCAM28). The two versions share the same overall model structure, but some hydrological processes and associated parameterisations are represented in a slightly simplified form in LASCAM22. The key differences between LASCAM22 and LASCAM28 are summarised in Appendix A.

In this study, LASCAM22 was run at a daily timestep using rainfall and potential evapotranspiration as climate inputs. These inputs are routed through a set of conceptual stores and fluxes to simulate streamflow at the catchment outlet. Note that some other versions of LASCAM also allow additional inputs, such as leaf area index (LAI) and the proportion of impervious area, to better represent land-use change and urbanisation.

https://doi.org/10.5194/egusphere-2026-4407
Preprint. Discussion started: 12 August 2026

The model structure consists of three conceptual stores: the A store, B store, and F store (Fig. 2). The A store represents the near-stream perching layer and riparian zone, the B store represents the deeper groundwater system, and the F store represents an unsaturated infiltration store (Ye et al., 1997). Following canopy interception losses, the remaining precipitation reaches the land surface as throughfall and is partitioned into surface and subsurface pathways, including infiltration, inter-store recharge, evaporation losses, saturation-excess runoff, infiltration-excess runoff, and discharge to the stream.

Table 1 provides the definitions, feasible ranges, and units of the 22 calibrated parameters used in LASCAM22. Full model equations are provided in Appendix B.

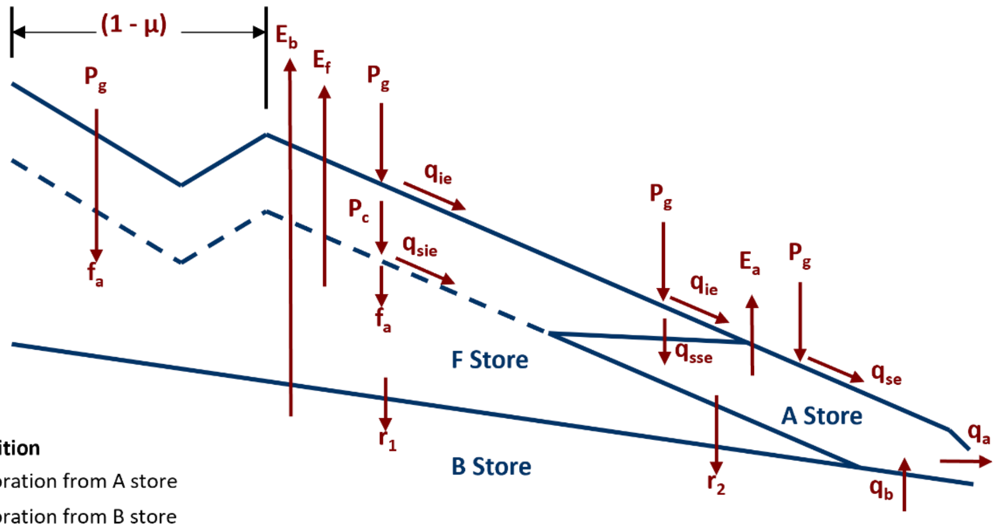

Symbol	Definition
E_a	Evaporation from A store
E_b	Evaporation from B store
E_f	Evaporation from F store
q_a	A store discharge to stream
q_b	B store discharge to A store
q_{se}	Saturation excess surface runoff
q_{ie}	Infiltration excess surface runoff
q_{sie}	Infiltration excess subsurface runoff
q_{sse}	Saturation excess subsurface runoff
P_g	Throughfall
P_c	Surface infiltration
f_a	Subsurface infiltration
r_2	Recharge from A store to B store
r_1	Recharge from F store to B store
μ	Upslope perching factor

Figure 2. Schematic of water fluxes and stores in LASCAM22.

https://doi.org/10.5194/egusphere-2026-4407
Preprint. Discussion started: 12 August 2026

Table 1. The definition, feasible range and units for each parameter in LASCAM22.

Parameters	Definition	Units	Min	Max
amn	A store reference minimum	mm/day	0	500
amx	A store reference maximum	mm/day	80	1000
bmx	B store reference maximum	mm/day	500	2500
fmx	F store reference maximum	mm/day	200	900
fs	Surface infiltration parameter	-	0.05	400
td	F store recharge parameter	-	1	1500
alphaa	A store discharge parameter	-	0.001	10
alphab	B store discharge parameter	-	0.001	10
alphac	Surface saturation parameter	-	0.0001	10
alphaf	Subsurface infiltration parameter	-	0.001	10
alphag	Throughfall parameter	-	-0.2	0.2
alphass	Subsurface saturation parameter	-	0.1	11
betaa	A store discharge parameter	-	0.01	10000
betab	B store discharge parameter	-	0.00001	10
betaf	Subsurface infiltration parameter	-	0.001	10
betag	Throughfall parameter	-	0	0.2
gammaa	A store evaporation parameter	-	0.001	10
gammab	B store evaporation parameter	-	0.1	1
gammaf	F store evaporation parameter	-	0.1	0.7
deltab	B store evaporation parameter	-	0.1	5
deltaf	F store evaporation parameter	-	0.3	1
mu	upslope perching parameter	-	0.01	0.99

4 Methods

4.1 Model simplification method

4.1.1 Overview

The simplification of LASCAM followed a stepwise process aimed at reducing calibration complexity while preserving the model's existing formulation. This was particularly important because LASCAM is currently used in water resource management applications in SWWA, where maintaining consistency with the operational model is desirable. Accordingly, simplification was implemented by fixing selected parameters at default values, rather than by removing stores, fluxes, or

https://doi.org/10.5194/egusphere-2026-4407
Preprint. Discussion started: 12 August 2026

other conceptual components. This strategy reduced the number of parameters requiring calibration while retaining the original model structure, thereby limiting the risk that simplification would cause substantial changes in simulated hydrological behaviour.

The workflow built on established sensitivity and calibration-based methods where possible (Fig. 3). Starting from LASCAM22, the method addressed three linked questions: (i) which parameters have low influence on model performance, analysed using Sobol sensitivity analysis (Sect. 4.1.2); (ii) can these low-sensitivity parameters be fixed at suitable default values, analysed using pairwise parameter sampling (Sect. 4.1.4); and (iii) how does model performance change as parameters are progressively fixed, analysed using stepwise parameter-fixing calibration (Sect. 4.1.5). The final simplified configuration was selected from the reduced-parameter configurations generated in Step 3, based on whether further parameter fixing led to meaningful performance loss relative to the reduction in calibration dimensionality.

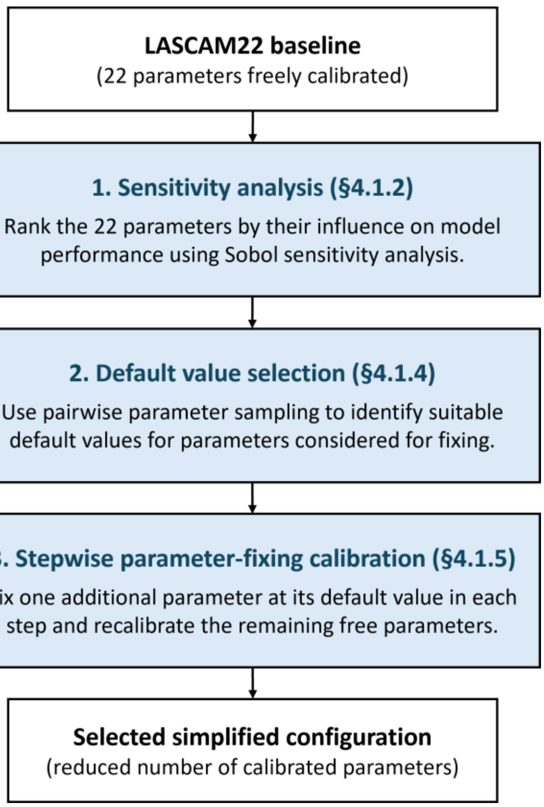

Figure 3. Overview of the LASCAM simplification workflow. Starting from the LASCAM22 baseline, the method included three steps: sensitivity analysis, default-value selection, and stepwise parameter-fixing calibration. The final simplified configuration was selected based on performance across the reduced-parameter configurations.

4.1.2 Step 1: Sensitivity analysis

The first step of the simplification framework was to identify which LASCAM22 parameters had limited influence on model performance. Sobol sensitivity analysis was used for this purpose because it provides a global assessment of parameter influence across the full parameter space and accounts for interactions among parameters (Saltelli et al., 2010). This was important for LASCAM because the model contains multiple interacting storage and flux processes, and parameter effects may therefore be nonlinear or dependent on the values of other parameters.

The Sobol method estimates how much of the variation in model performance can be attributed to each parameter. Parameter influence was ranked using the total-order Sobol index, which accounts for both the direct effect of each parameter and its interactions with other parameters. Parameters with consistently low total-order indices across catchments were considered to have limited influence on model performance and were therefore treated as candidates for fixing in later simplification steps (Sect. 4.1.4).

In this study, the sampling size was chosen to balance the stability of the sensitivity estimates with the computational cost of running LASCAM22. This resulted in approximately 150,000 model realisations, with each realisation evaluated using the bounded Trotter score as the objective function (described in Sect. 4.1.3).

4.1.3 Performance metrics and objective functions

Model performance was evaluated using Trotter-based metrics, with NSE-Bias and percent bias (PBIAS) used as supplementary checks on bias-penalised efficiency and volumetric error (Table 2). The Trotter score was used as the base metric because it combines performance for untransformed streamflow, low-flow behaviour, and volumetric bias into a single measure (Trotter et al., 2023):

$$Trotter = \frac{1}{2}\left(KGE_Q + KGE_{Q^{0.2}}\right) - 5 \cdot |\ln(B+1)|^{2.5} \quad (1)$$

where KGE_Q is the Kling-Gupta efficiency (KGE; Gupta et al., 2009) based on untransformed streamflow, $KGE_{Q^{0.2}}$ is the KGE based on the fifth root transformed streamflow, and B denotes the volumetric bias between simulated and observed streamflow.

Two Trotter-based formulations were used for different parts of the workflow. Bounded Trotter was used for the Sobol sensitivity analysis because raw Trotter values can become very large magnitude negative numbers, which may dominate variance-based sensitivity estimates. Trotter scores were therefore transformed to the bounded range (-1, 1) using the C2M transformation of Mathevet et al. (2006):

$$Bounded\ Trotter = \frac{Trotter}{2 - Trotter} \quad (2)$$

https://doi.org/10.5194/egusphere-2026-4407
Preprint. Discussion started: 12 August 2026

Split-Trotter was used for calibration-based experiments because it reduces the tendency for calibration procedures to prioritise wetter years at the expense of dry-year performance (Fowler et al., 2018a), by calculating the Trotter separately for each year and then averaging across years:

$$Split\ Trotter = \frac{\sum_{i=1}^{NumYears} Trotter_i}{\sum NumYears} \quad (3)$$

Note that Split-Trotter was not used in the Sobol sensitivity analysis because calculating annual Trotter scores for every Sobol model evaluation would substantially increase computational cost. Bounded Trotter was therefore used as a practical alternative for parameter ranking, with the later calibration experiments using Split-Trotter to test the effect of fixing low-sensitivity parameters.

We also calculated NSE-Bias as a supplementary metric, which was calculated by combining the Nash-Sutcliffe Efficiency (NSE) with the same volumetric bias penalty used in the Trotter score, which was originally proposed by Viney et al. (2009):

$$NSE\ Bias = NSE - 5 \cdot |\ln(B+1)|^{2.5} \quad (4)$$

PBIAS is another supplementary metric, mainly used in the split sample test (Sect. 4.2). It directly measures volumetric bias, which is important for water resource applications where systematic over- or under-estimation of total streamflow can affect estimates of water availability. PBIAS was calculated as:

$$PBIAS(\%) = \frac{\sum_{i=1}^{n}(Q_{sim,i} - Q_{obs,i})}{\sum_{i=1}^{n} Q_{obs,i}} \times 100 \quad (5)$$

Table 2. Objective functions and supplementary metrics used in the LASCAM simplification and evaluation workflow.

Metric / Objective function	Used in	Reason for use
Bounded Trotter	Sobol sensitivity analysis (Sect. 4.1.2)	Provides a bounded output for variance-based sensitivity analysis and avoids very large negative Trotter values dominating sensitivity estimates.
Split Trotter	Default-value selection (Sect. 4.1.4); Stepwise parameter-fixing calibration (Sect. 4.1.5); Split sample test (Sect. 4.2)	Gives each year equal weight, reducing the tendency for calibration to be dominated by wet years.
NSE Bias	Stepwise parameter-fixing calibration (Sect. 4.1.5); Split sample test (Sect. 4.2)	Provides a bias-penalised NSE-based check on model performance.
PBIAS	Split sample test (Sect. 4.2)	Directly quantifies volumetric over- or under-estimation of total streamflow.

https://doi.org/10.5194/egusphere-2026-4407
Preprint. Discussion started: 12 August 2026

4.1.4 Step 2: Default-value selection

Step 2 identified suitable default values for the low-sensitivity parameters identified in Step 1, before their effect was tested through stepwise parameter-fixing calibration in Step 3. We did not take these values directly from the optimised values for LASCAM22 for any single catchment, because the aim was to identify values that were broadly suitable across a variety of catchments. Instead, default values were selected using pairwise parameter sampling and behavioural regions across catchments. The overall logic of this section is that the parameters to be fixed and the values to which they are fixed should be chosen based on evidence that the fixing can be compensated for by another parameter that is still free. The method is thus focussed on seeking and collating this evidence across catchments. The procedure is summarised in Fig. 4.

The first part of the procedure used the Sobol sensitivity ranking results to define two parameter groups for pairwise testing (Fig. 4a). Parameters at the lower end of the sensitivity ranking (i.e., least sensitivity) were considered for fixing and paired with a remaining (i.e., free) parameter.

Pairwise sampling was then conducted only across these two groups (Fig. 4b). For each catchment, an optimised parameter set from the LASCAM22 calibration was used as the reference parameter set, with the calibration procedure described in Sect. 4.1.5. For each cross-group parameter pair, the two selected parameters were varied across their allowed ranges, while the remaining 20 parameters were fixed at their calibrated LASCAM22 values for that catchment. Each pair was sampled using 50 values for each parameter, giving a 50 × 50 grid of 2,500 parameter combinations. Note that sampling was conducted on the original parameter scale for most parameters, but in log space for parameters whose upper bound was more than 1000 times larger than the lower bound.

Behavioural samples were retained from each pairwise sample grid. A sampled combination was classified as behavioural if it fell within the top 5% of model realisations for that parameter pair and achieved at least 80% of the LASCAM22 optimum for the corresponding catchment. These criteria retained parameter combinations that performed well relative to the catchment-specific baseline, while allowing some flexibility around the optimum.

The behavioural samples were then compared across catchments to select default values (Fig. 4c). For each parameter being considered for fixing, we searched for a value that lay within a stable behavioural region across most catchments when paired with one retained calibrated parameter. This indicated that the parameter could be fixed at a shared value without compromising performance in any of the catchments tested. Where no robust default value could be identified, the parameter was kept free initially and moved later in the fixing order. This reduced the risk that unsuitable default values would cause performance loss during the early stages of the stepwise fixing experiment.

https://doi.org/10.5194/egusphere-2026-4407
Preprint. Discussion started: 12 August 2026

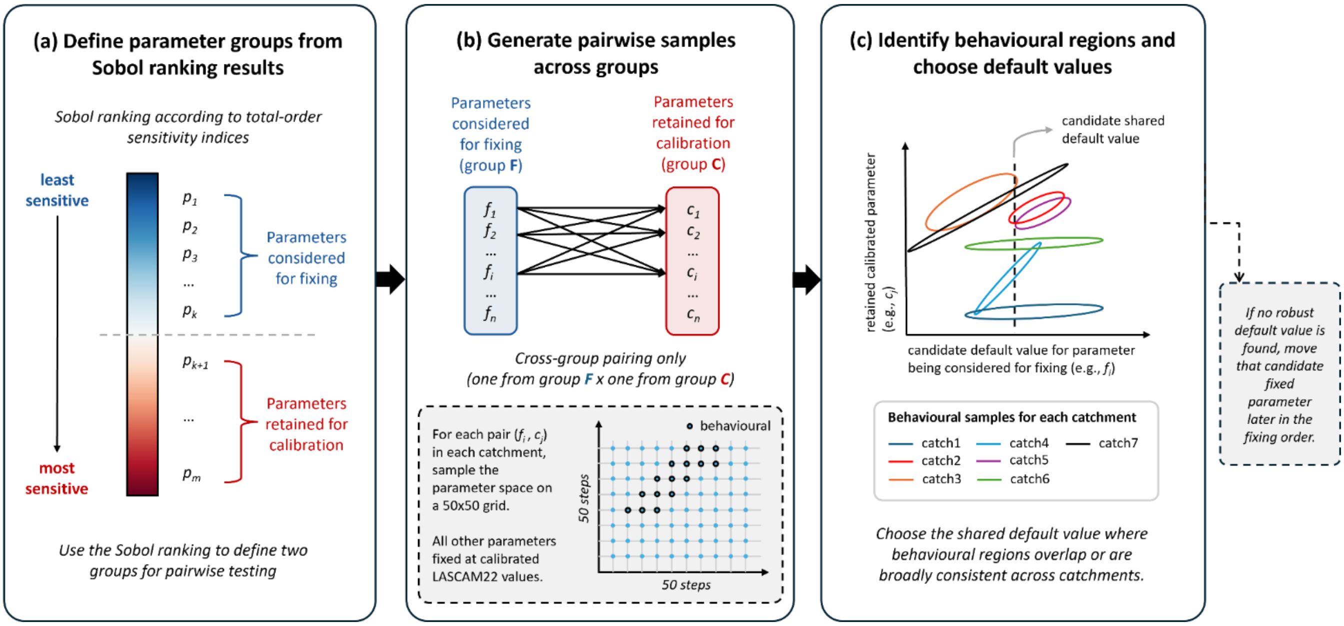

Figure 4. Procedure used to select default values based on intersection of behavioural regions across catchments. The overall idea is that parameters to be fixed and the values to which they are fixed should be chosen based on evidence that the fixing can be compensated for by another parameter that is still free. (a) The Sobol sensitivity ranking was used to define two parameter groups for pairwise testing: parameters considered for fixing and parameters retained for calibration. (b) Pairwise sampling was conducted across these groups, and behavioural samples were identified for each parameter pair. (c) Behavioural regions were then compared across catchments to select shared default values. A shared default value indicated that the paired parameter could compensate across all catchments.

4.1.5 Step 3: Stepwise parameter-fixing calibration

Step 3 tested whether the low-sensitivity parameters could be fixed at their selected default values without substantially degrading model performance. After assigning default values to the candidate fixed parameters in Step 2, we evaluated their effect through a baseline calibration followed by a sequence of reduced-parameter recalibrations.

The baseline used LASCAM22 for each study catchment and provided the performance reference against which the reduced-parameter calibrations were compared. Using this baseline as the reference, we then evaluated the effect of fixing low-sensitivity parameters through a stepwise recalibration procedure (Fig. 5). Candidate fixed parameters were fixed one at a time, beginning with the least sensitive parameter according to the final fixing order and using the default values identified in Step 2. The procedure was cumulative, meaning that parameters fixed in earlier steps remained fixed in later steps. After each fixing step, we recalibrated the model using only the remaining free parameters. This reduced the number of calibrated parameters by one at each step and generated a sequence of reduced-parameter configurations. For example, the 21-parameter model fixed only the least sensitive parameter, while the 20-parameter model fixed the two least sensitive parameters.

The LASCAM22 baseline calibration also provided the reference parameter sets used in the pairwise sampling procedure described previously. For each candidate model, calibration was conducted using all available data from the corresponding

https://doi.org/10.5194/egusphere-2026-4407
Preprint. Discussion started: 12 August 2026

catchment. A warmup period of 30 years was used to allow sufficient time for slow-responding model stores, particularly the deep groundwater storage (B store), to equilibrate prior to performance evaluation (Zhang et al., 2026).

We adopted the Covariance Matrix Adaptation Evolution Strategy (CMA-ES) as the optimisation algorithm, following the recommendation of Arsenault et al. (2014), due to its strong performance in calibrating hydrological models with large parameter spaces and complex parameter interactions. To reduce the risk of convergence to local optima, we repeated the calibration 30 times for each catchment, each time with different random seeds. The parameter set yielding the highest objective function value was retained for each configuration.

At each fixing step, model performance was evaluated using the Split-Trotter objective function and compared with the corresponding LASCAM22 baseline, with NSE-Bias used as a supplementary performance metric. A reduced-parameter configuration was considered acceptable if fixing parameters caused little or no decline in model performance. Note that the above procedure was applied to all catchments in the wider sample, even though the process depicted in Fig. 4 was only undertaken for the seven primary catchments.

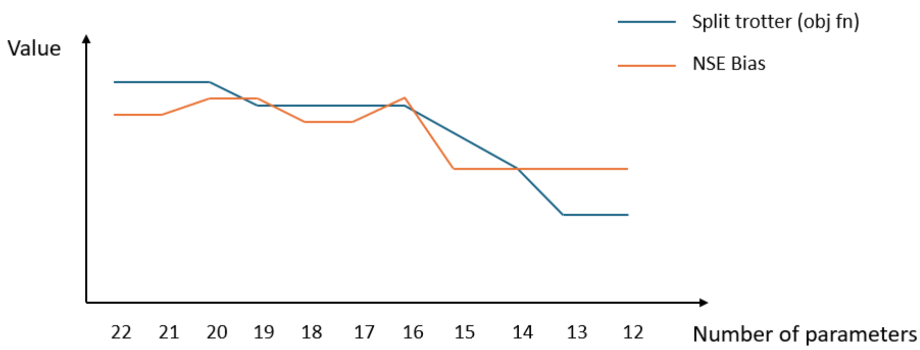

Figure 5. Schematic example of the stepwise fixing with recalibration process. Beginning with LASCAM22, low-sensitivity parameters are progressively fixed, leaving a reduced number of free parameters. At each step, the remaining parameters are recalibrated using the Split-Trotter as objective function and model performance is also assessed using NSE-Bias.

4.2 Evaluation framework for adopted model

After selecting the simplified LASCAM, we evaluated it and LASCAM22 using a split-sample test. GR4J and Sacramento were also included as reference models, providing context for interpreting LASCAM performance relative to other rainfall-runoff models commonly used in Australia. This evaluation assessed model performance outside the calibration period using the wider catchment sample. Note that all calibrations were to a single catchment at a time (i.e. no regional or multi-catchment calibrations were undertaken).

For each catchment and model, calibration was performed using runoff observations before 2011, and validation was conducted using runoff observations from 2011 onwards. The period after 2011 was typically drier than the preceding period. The models were run continuously across the available record, with performance calculated separately for the calibration and validation periods. The calibration settings followed those described in Sect. 4.1.5.

https://doi.org/10.5194/egusphere-2026-4407
Preprint. Discussion started: 12 August 2026

The split-sample test was not used to select the simplified LASCAM configuration, because its results can depend on how the available record is divided into calibration and validation periods. We also acknowledge that other split-sample designs are possible, including bootstrap-based resampling, odd-even year splits, and differential split-sample tests (e.g., Arsenault et al., 2018; Coron et al., 2012; Essou et al., 2016; Klemeš, 1986). Here, we used a single chronological split to provide a consistent final evaluation across the wider catchment sample, and the simplified configuration was selected using the analyses described in Sect. 4.1.

5 Results

5.1 Sobol sensitivity ranking

The Sobol sensitivity analysis indicated that the influence of the 22 LASCAM parameters was highly uneven, with sensitivity concentrated in a small subset of parameters (Fig. 6). The total-order sensitivity ranking identified *amn* as the most influential parameter on average across the seven primary catchments, while *alphag* showed the lowest average sensitivity.

Although the overall ranking was not identical across all catchments, the group of low-sensitivity parameters was broadly consistent. Based on the average total-order ranking, the ten lowest-ranked parameters were selected as the initial group considered for fixing: *alphag*, *betaa*, *alphac*, *gammab*, *alphass*, *betab*, *deltaf*, *bmx*, *deltab*, and *betaf*. The remaining 12 parameters were retained for calibration during the pairwise default-value testing. This 10:12 split was used as a practical starting point rather than a hard sensitivity threshold. It captured the parameters with consistently small total-order effects while testing a substantial potential reduction in calibration dimensionality from 22 to 12.

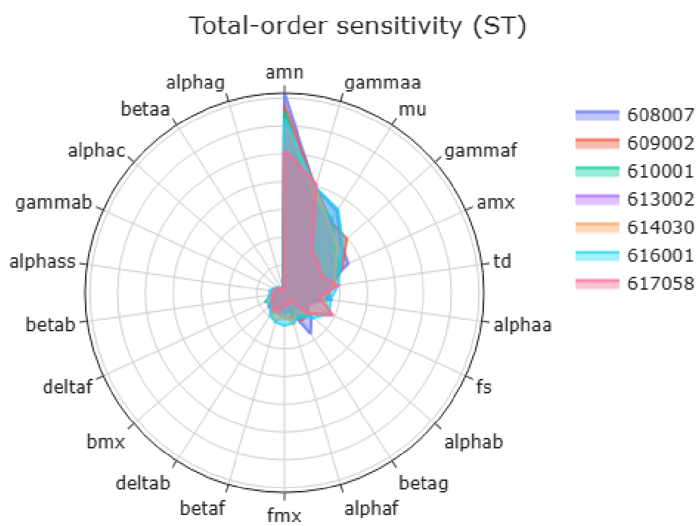

Figure 6. Total-order Sobol sensitivity indices (ST) for the 22 LASCAM parameters across the seven primary catchments, ranked from the top axis (0°) clockwise by average sensitivity, showing strongest sensitivity to *amn* and broadly consistent low-sensitivity parameters across catchments.

https://doi.org/10.5194/egusphere-2026-4407
Preprint. Discussion started: 12 August 2026

5.2 Parameter pairings and default values

The pairwise behavioural analysis identified robust pairings and default values for seven of the ten candidate fixed parameters (Table 3), indicating potential for fixing these parameters with minimal loss in performance. For these parameters, the behavioural samples showed overlapping acceptable range across most or all of the seven primary catchments, suggesting that the paired parameter could compensate regardless of the catchment, provided the default value was chosen to be in that range (e.g., *alphac* can be fixed at 1 as shown in Fig. 7a and 7b). In cases where overlap was not achieved across all seven catchments, the result was interpreted with some flexibility, because the overlap depends partly on the criteria used to define behavioural samples (Sect. 4.1.4). For example, the *deltaf* - *gammaf* pair showed overlap across six catchments, with the remaining catchment (617058) located close to the overlapping region (Supplement Fig. S6). This suggests that a slightly less restrictive behavioural threshold may have produced overlap across all seven catchments. In such cases, the selected default value was chosen from within the main overlapping range, but positioned closer to the behavioural range of the non-overlapping catchment where possible.

Table 3. Parameter pairings, adopted default values, and adjusted fixing order for the ten candidate fixed parameters.

Candidate fixed parameter	Sobol sensitivity rank	Adopted default value	Paired retained parameter	Adjusted fixing order
alphag	22	-0.14	*betag*	1
betaa	21	50	*alphaa*	2
alphac	20	1	*mu*	3
gammab	19	/	/	8
alphass	18	8	*td*	4
betab	17	0.5	*alphab*	5
deltaf	16	0.5	*gammaf*	6
bmx	15	2500	*alphaf*	7
deltab	14	/	/	9
betaf	13	/	/	10

In contrast, no robust default value could be identified for *gammab, deltab and betaf*. Across the tested pairings, several catchments showed incompatible behavioural regions, which means no single value could satisfy most catchments simultaneously. For example, in Fig. 7c and 7d, the acceptable range of *gammab* differs largely between the two catchments, indicating limited overlap and no robust default value could be assigned for *gammab*. Although *gammab* was ranked as a relatively low-sensitivity parameter (Fig. 6), it was moved later in the fixing order to avoid fixing it early at a poorly supported value. The same reasoning was applied to *deltab* and *betaf*.

https://doi.org/10.5194/egusphere-2026-4407
Preprint. Discussion started: 12 August 2026

The pairwise analysis also suggested that the original upper bounds for *bmx* and *td* may have been restrictive (Supplement Figs. S4 and S7). Behavioural samples for these parameters tended to occur near the upper end of their feasible ranges, indicating that larger values may be appropriate in future calibration experiments. Full pairwise behavioural analysis results are provided in the Supplement S1.

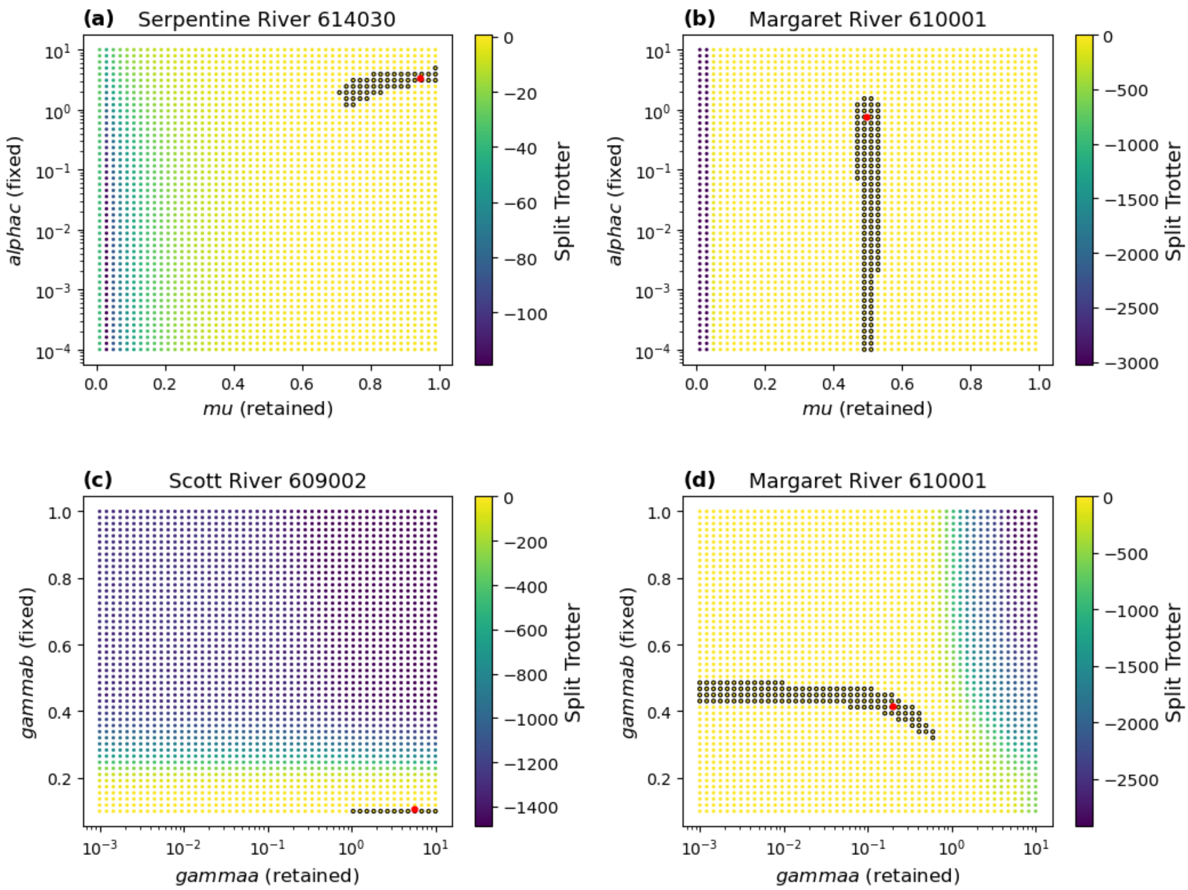

Figure 7. Example pairwise behavioural analysis for candidate fixed parameters across catchments. The top row shows *alphac* paired with *mu* for catchments (a) Serpentine River and (b) Margaret River, while the bottom row shows *gammab* paired with *gammaa* for (c) Scott River and (d) Margaret River. The red point represents the baseline optimum (Sect. 4.1.5), and black-edged points indicate behavioural parameter samples satisfying the selection criteria. The top row suggests relatively high potential to assign *alphac* = 1, whereas the bottom row shows limited overlap in acceptable *gammab* values, indicating that no robust default could be assigned for *gammab*.

5.3 Sequential parameter-fixing calibration

As explained in Sect. 4.1.5, the 22-parameter configuration represents the baseline calibration, where all parameters were freely calibrated. Each subsequent configuration fixed one additional parameter according to the fixing order in Table 3 and recalibrated the remaining free parameters. For example, the 21-parameter configuration fixed the first fixing parameter, *alphag*, at its adopted default value of -0.14, while the remaining 21 parameters were recalibrated. This process continued across other parameters in a cumulative fashion using the adjusted fixing order from Table 3. Although robust default values

https://doi.org/10.5194/egusphere-2026-4407
Preprint. Discussion started: 12 August 2026

could not be identified for *gammab*, *deltab*, or *betaf*, provisional values were assigned for the purposes of testing these parameters in the full stepwise calibration procedure. Specifically, *gammab* was fixed at 0.2, *deltab* at 0.3, and *betaf* at 3, with these values selected to fall within the behavioural regions observed across the tested pairings.

Across the 76 catchments, the distribution of Split-Trotter values remained broadly similar as the number of calibrated parameters was reduced from 22 to 14 (Fig. 8). The median Split-Trotter declined gradually as more parameters were fixed, but the reduction between the 22-parameter baseline and the 14-parameter configuration remained below 0.1. The spread and median drop became larger in the 13- and 12-parameter configurations, suggesting that extending the reduction beyond 14 calibrated parameters caused a more noticeable loss of performance. This decline coincided with fixing *deltab* and *betaf*, for which robust default values could not be identified in the parameter-pairing results. NSE-Bias showed a similar gradual reduction in median performance, with a median decline of less than 0.1 up to the 14-parameter configuration. However, the spread in NSE-Bias was more stable only up to the 15-parameter configuration, suggesting that the 15-parameter configuration provides a slightly more robust simplification when both performance metrics are considered.

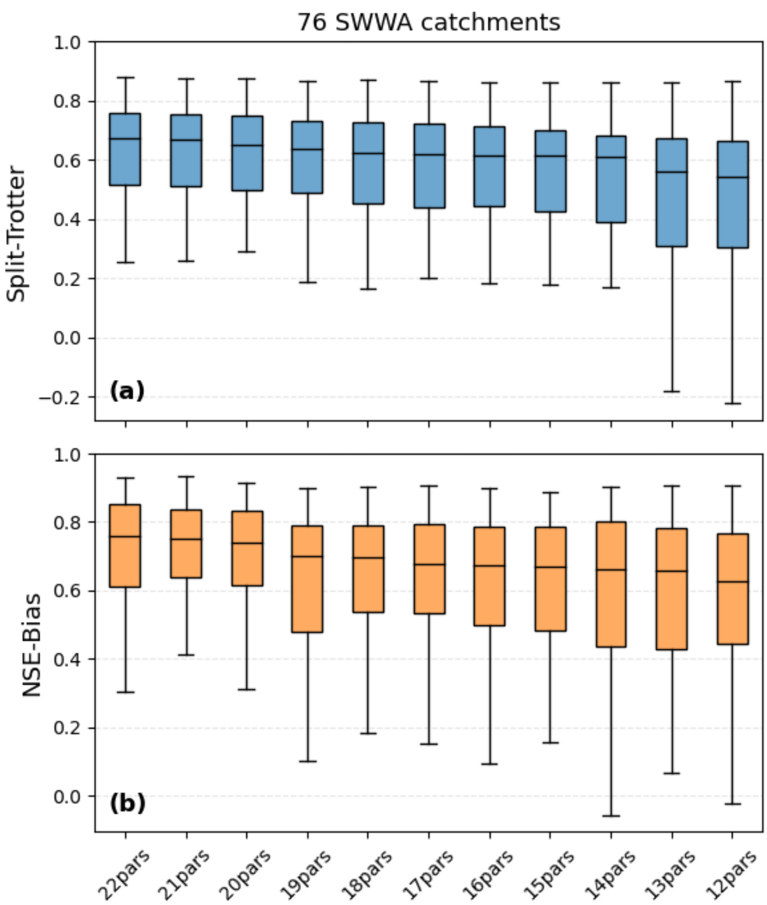

Figure 8. Distribution of (a) Split-Trotter and (b) NSE-Bias across the 76 SWWA catchments for each reduced-parameter LASCAM configuration.

https://doi.org/10.5194/egusphere-2026-4407
Preprint. Discussion started: 12 August 2026

The spatial results further show that the effect of parameter reduction was largely consistent with the baseline performance pattern (Fig. 9). Catchments that performed relatively poorly under the 22-parameter baseline generally continued to perform poorly under the simplified configurations (e.g., consistently red catchments), while catchments with stronger baseline performance tended to remain better performing after simplification. This suggests that the simplified configurations did not substantially alter the spatial pattern of model performance; instead, much of the variation appears to reflect catchment-specific modelling difficulty already present in the baseline model. The corresponding NSE-Bias results are consistent with this interpretation (Supplement Fig. S8).

Overall, the sequential parameter-fixing results support reducing LASCAM from 22 to 15 calibrated parameters as a robust simplification, with limited loss of performance across the study catchments. The 14-parameter configuration also remained viable and may be acceptable where stronger dimensionality reduction is required, but the larger spread in NSE-Bias at 14 parameters indicates that retaining 15 calibrated parameters provides a more stable compromise between parsimony and performance retention.

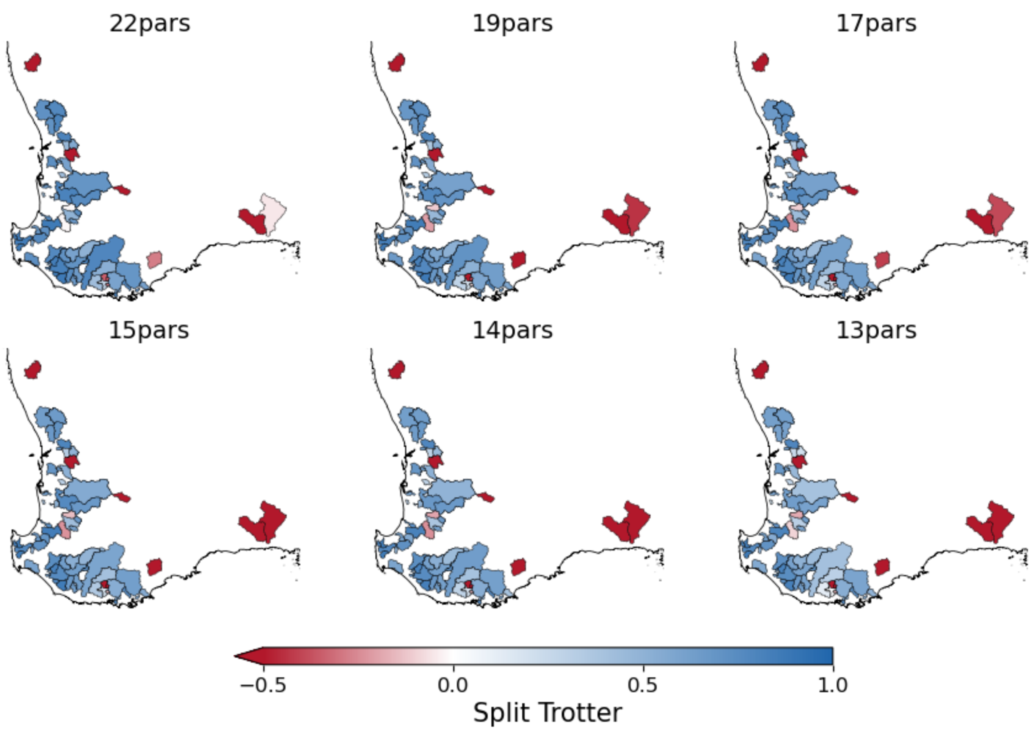

Figure 9. Spatial distribution of Split-Trotter values for selected LASCAM configurations (22-, 19-, 17-, 15-, 14- and 13-parameter) across the 76 SWWA catchments. Colours indicate Split-Trotter performance, with blue representing higher values and red representing lower (negative) values.

https://doi.org/10.5194/egusphere-2026-4407
Preprint. Discussion started: 12 August 2026

5.4 Final adopted reduced LASCAM configuration

Based on the sequential parameter-fixing calibration results, the 15-parameter configuration was adopted as the final reduced version of LASCAM. This configuration provided a robust compromise between reducing calibration dimensionality and retaining model performance across the study catchments. The fixed and calibrated parameters in the adopted LASCAM15 configuration are listed in Table 4 (note that Sect. 6.1 discusses these fixed parameters with respect to catchment processes). The adopted LASCAM15 configuration was then used in the split-sample test to evaluate whether the reduced model retained robust performance under independent calibration and evaluation periods.

Table 4. Parameter specification of the adopted LASCAM15 configuration. The table lists the LASCAM22 parameters, their status in LASCAM15, fixed default values where applicable, and calibration ranges for parameters retained for calibration. Note that Sect. 6.1 discusses these fixed parameters with respect to catchment processes.

Parameters	Definition	Status	Defaults	Min	Max
amn	A store reference minimum [mm/day]	calibrated		0	500
amx	A store reference maximum [mm/day]	calibrated		80	1000
fmx	F store reference maximum [mm/day]	calibrated		200	900
fs	Surface infiltration parameter	calibrated		0.05	400
td	F store recharge parameter	calibrated		1	1500[a]
alphaa	A store discharge parameter	calibrated		0.001	10
alphab	B store discharge parameter	calibrated		0.001	10
alphaf	Subsurface infiltration parameter	calibrated		0.001	10
betaf	Subsurface infiltration parameter	calibrated		0.001	10
betag	Throughfall parameter	calibrated		0	0.2
gammaa	A store evaporation parameter	calibrated		0.001	10
gammab	B store evaporation parameter	calibrated		0.1	1
gammaf	F store evaporation parameter	calibrated		0.1	0.7
deltab	B store evaporation parameter	calibrated		0.1	5
mu	upslope perching parameter	calibrated		0.01	0.99
bmx	B store reference maximum [mm/day]	fixed	2500[a]		
alphac	Surface saturation parameter	fixed	1		
alphag	Throughfall parameter	fixed	-0.14		
alphass	Subsurface saturation parameter	fixed	8		
betaa	A store discharge parameter	fixed	50		
betab	B store discharge parameter	fixed	0.5		
deltaf	F store evaporation parameter	fixed	0.5		

[a]These values were identified as potentially expandable based on the calibration results.

https://doi.org/10.5194/egusphere-2026-4407
Preprint. Discussion started: 12 August 2026

5.5 Split sample test

The split-sample test further supported the robustness of the adopted LASCAM15 configuration (Fig. 10). Although LASCAM15 showed a small reduction in calibration performance compared with LASCAM22, LASCAM15 performed better than LASCAM22 in validation, with higher median performance and a narrower spread for the main metrics. This result suggests that the reduced parameter set was not only computationally simpler, but also transferred well to an independent validation period. Both LASCAM configurations also continued to outperform GR4J and Sacramento, demonstrating the stronger robustness of the LASCAM structure under independent evaluation conditions.

Although it is pleasing that LASCAM22 outperformed the other models, all models tested performed poorly overall, consistent with prior split sample tests conducted in Australia (e.g., Fowler et al., 2018a). Performance declined substantially for all models during the post-2011 validation period, showing that this period provided a challenging out-of-sample test. Furthermore, GR4J and Sacramento attained poor scores even in calibration (relative to the LASCAM variants), with median Split Trotter scores of 0.4 and 0.5, respectively, and median NSE-bias scores of 0.72 and 0.68, respectively. The lower scores for Split Trotter may be because the performance in every year is weighted equally, pulling down the overall score, which is not the case for the NSE-bias objective function.

Overall, the split-sample results show that LASCAM15 provides a strong compromise between model performance, robustness, and computational efficiency. It retains most of the calibration strength of LASCAM22, performs better than GR4J and Sacramento in both calibration and validation, and most importantly it outperforms its parent model in validation in the context of split sample testing on a period that is significantly drier. This last result is particularly important for the management context the model is intended to support, in which a persistent drying has occurred and is expected to intensify in future.

https://doi.org/10.5194/egusphere-2026-4407
Preprint. Discussion started: 12 August 2026

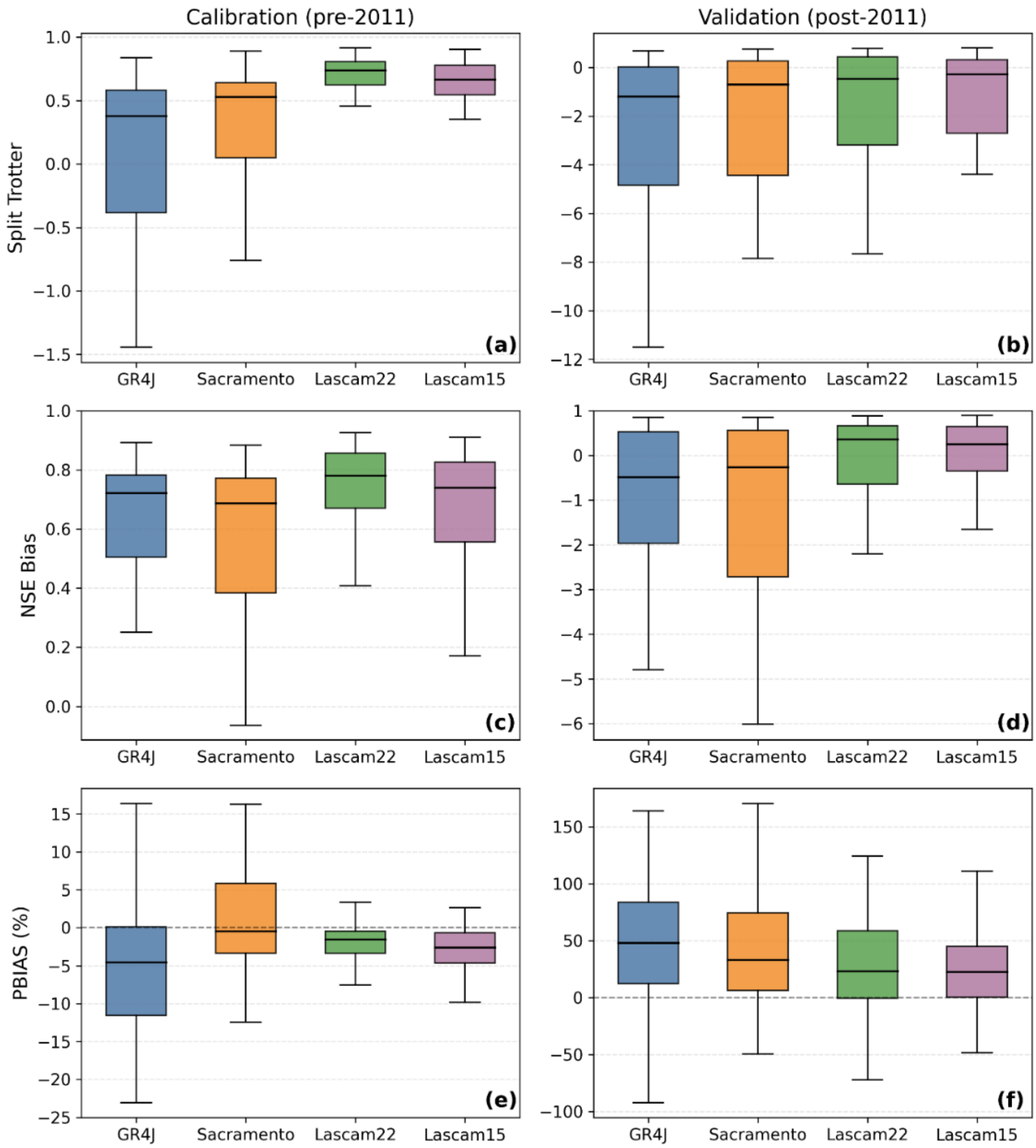

400 **Figure 10.** Split-sample test results for GR4J, Sacramento, LASCAM22, and the adopted LASCAM15 configuration across the 76 wider sample of catchments. Panels show Split-Trotter (a, b), NSE-Bias (c, d), and PBIAS (e, f) during the pre-2011 calibration period and post-2011 validation period.

https://doi.org/10.5194/egusphere-2026-4407
Preprint. Discussion started: 12 August 2026

6 Discussion

6.1 Parameter sensitivity and implications for LASCAM structure

The main implication of the simplification results is that much of the LASCAM's calibration burden could be reduced without changing the model's core hydrological structure. The parameters fixed in LASCAM15 were mainly associated with scaling, offset, or curvature terms within existing LASCAM flux equations, rather than with the removal of major hydrological pathways. This distinction is important: fixing a parameter does not mean that the related process is removed from the model. Instead, the process remains active, but one degree of freedom in how that process varies between catchments is constrained using a default value. In LASCAM15, throughfall adjustment, surface and subsurface saturation-excess runoff, A- and B-store discharge, and F-store evaporation are all retained, but selected components of their parameterisation are fixed (Table 5). More specifically, fixing parameters such as *alphaq*, *alphac*, and *alphass* constrains baseline throughfall and the rate at which saturated areas expand, but the corresponding runoff-generation pathways remain represented. Similarly, fixing *betaa* and *betab* reduces flexibility in the magnitude scaling of A- and B-store discharge, while other parameters controlling store behaviour and relative response remain calibrated. In this sense, the simplified model preserves the main water balance structure while reducing parameter freedom in parts of the model that previously over parameterised.

The sensitivity results should therefore be interpreted as evidence of limited parameter identifiability rather than physical irrelevance. Some fixed parameters may still represent meaningful hydrological controls, but their catchment-specific values were either secondary for streamflow simulation, partly compensated by other calibrated parameters, or very similar across the SWWA catchments considered here. This supports the use of LASCAM15 as a structurally conservative simplification: calibration dimensionality is reduced, but the main stores and flux pathways of the original LASCAM structure are retained.

https://doi.org/10.5194/egusphere-2026-4407
Preprint. Discussion started: 12 August 2026

Table 5. Process interpretation of parameters fixed in the adopted LASCAM15 configuration.

Fixed parameter	Role in the flux equations	Remaining flexibility in LASCAM15 and interpretation
alphag	Controls the additive component of the throughfall relationship, before rainfall is converted to effective throughfall (Appendix B, Eq. B1).	Throughfall adjustment is retained because *betag* remains calibrated, but one degree of freedom in the rainfall-to-throughfall conversion is fixed.
bmx	Defines relative B-store storage, which is then used in B-store discharge, B-store evaporation, and subsurface infiltration capacity (Appendix B, Eqs. B4, B11, B23, B25).	Slow-storage dynamics are retained because *alphab*, *gammab*, *deltab*, and related B-store flux controls remain calibrated, but the storage-capacity scaling of the B store is fixed.
alphac	Controls the surface saturated-area fraction, which determines the portion of throughfall contributing to surface saturation-excess runoff and infiltration partitioning (Appendix B, Eqs. B8, B9, B10, B12, B13, B14).	The surface runoff pathway remains active, but calibrated flexibility in surface saturated-area expansion is reduced.
alphass	Controls the subsurface saturated-area fraction, which affects subsurface saturation-excess runoff, infiltration partitioning and recharge from A store to B store (Appendix B, Eqs. B7, B13, B14, B17).	The subsurface saturation mechanism is retained, but its saturated-area scaling is fixed.
betaa	Scales discharge from the A store, which contributes directly to simulated streamflow (Appendix B, Eq. B6).	Fast/intermediate runoff response from the A store is retained because *alphaa* remains calibrated, but one discharge-scaling degree of freedom is fixed.
betab	Scales discharge from the B store, which contributes to slower storage-controlled water movement (Appendix B, Eq. B23).	Slow-store discharge remains represented because *alphab* remains calibrated, but one discharge-scaling degree of freedom is fixed.
deltaf	Controls the curvature of the relationship between relative F-store storage and F-store evaporation limitation (Appendix B, Eq. B21).	F-store evaporation remains active because *gammaf* remains calibrated, but the storage-dependent shape of this evaporation response is fixed.

435

https://doi.org/10.5194/egusphere-2026-4407
Preprint. Discussion started: 12 August 2026

6.2 Retention of vegetation water use and long-term storage processes in LASCAM15

Beyond overall streamflow performance, an important question is whether LASCAM15 retains the process features that motivated the use of LASCAM in the first place. Previous work showed that LASCAM has strengths in representing both evapotranspiration behaviour and longer-term storage dynamics. Burns et al. (2025) showed that the evapotranspiration formulation used in LASCAM matches flux tower AET better because Australian AET commonly remains permanently below PET (even under optimal moisture) and the LASCAM formulation suits this because it avoids the common assumption that AET always equals PET under moist conditions. This reduces over-extraction of water and better captures the dynamics between soil moisture and evapotranspiration. For this reason, two features are particularly important: the ability to restrict AET below PET even under high soil moisture conditions, and the concave non-linear relationship between AET and relative soil moisture which makes AET less sensitive to soil moisture changes.

These features are largely retained in LASCAM15. For B store (the deep groundwater store), the evapotranspiration formulation remains unchanged, with both *deltab* and *gammab* retained as calibrated parameters. This means that both the curvature of the soil moisture-AET relationship and the control that allows AET to remain below PET are preserved as catchment-specific degrees of freedom. For the F store, *deltaf* is fixed, which standardises the curvature of the F-store evaporation response, but *gammaf* remains calibrated. Therefore, the simplified model still retains the ability to limit AET below PET, although one aspect of the dynamic soil moisture-evapotranspiration relationship is constrained.

LASCAM15 also retains the structural features previously identified as important for representing multi-annual storage dynamics. Zhang et al. (2026) showed that LASCAM satisfied all the three structural components for capturing longer-term storage behaviour, and these components are preserved in LASCAM15 because no stores or major flux pathways were removed. The simulated B-store storage in Record Brook (608007) provides an example of this continuity (Fig. 11a). Although LASCAM15 and LASCAM22 do not produce identical absolute B-store storage values, this is not required because the B-store is a conceptual storage state whose magnitude depends on the calibrated parameter set. The more important comparison is whether the reduced model preserves the temporal behaviour and low frequency dynamics of the deep-storage system. In this case, LASCAM15 follows a similar seasonal cycle and long-term declining trajectory to LASCAM22, indicating that the reduced configuration retains the broad deep-storage dynamics of the 22-parameter baseline.

This storage behaviour is also broadly consistent with the available groundwater observations near Record Brook (e.g., the Lewin North control groundwater bores, Fig. 11b). Although monitoring was mostly discontinued after 1994 and only resumed sporadically after 2016, the Lewin North control bores show much lower groundwater level in the recent record than during the earlier monitoring period (George et al., 2025). This observed long-term decline is consistent with the declining B-store storage simulated by both LASCAM22 and LASCAM15. This provides supporting evidence that both configurations can represent the multi-annual storage dynamics observed in the region, and that LASCAM15 retains this long-term memory behaviour despite its reduced parameter dimensionality.

https://doi.org/10.5194/egusphere-2026-4407
Preprint. Discussion started: 12 August 2026

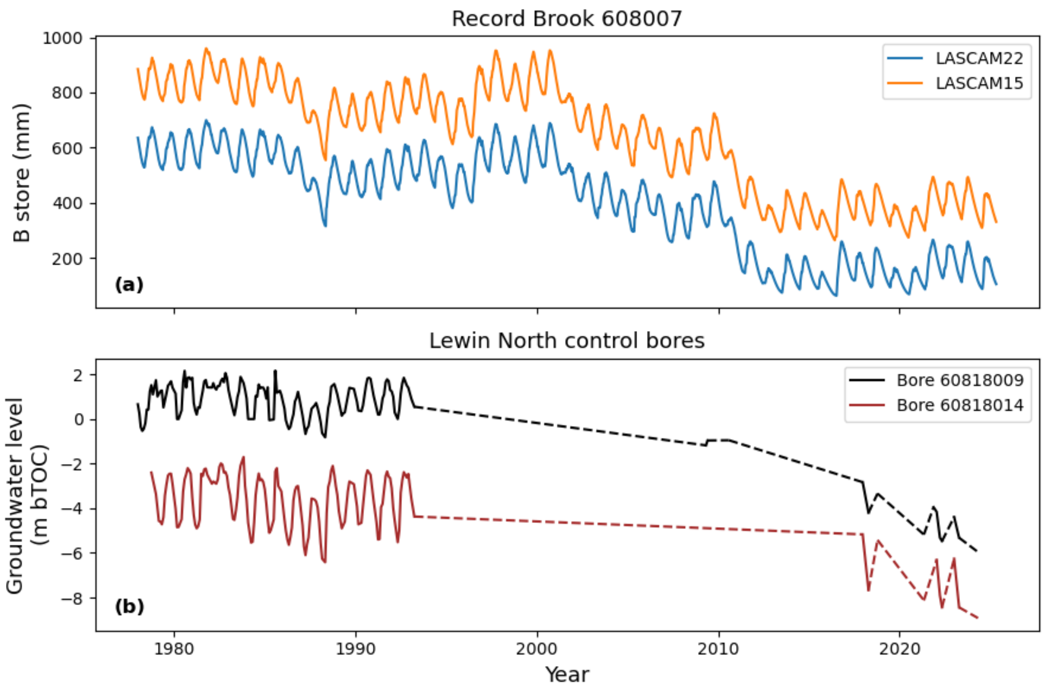

Figure 11. Comparison of simulated deep groundwater dynamics and observed groundwater levels near Record Brook (608007). Panel (a) shows simulated B-store storage from LASCAM22 and LASCAM15. Panel (b) shows groundwater levels from the Lewin North control bores, adapted from George et al. (2025). Gaps in the groundwater record longer than 180 days are shown as dashed lines.

6.3 Extrapolating hydrological models to future conditions

The split-sample test results support LASCAM15 as a robust reduced configuration, but they also show that extrapolating rainfall-runoff models to drier conditions remains difficult. In the post-2011 validation period, LASCAM15 performed better than LASCAM22, GR4J, and Sacramento, indicating that the reduced configuration transferred well relative to the other models tested. However, all models showed lower validation performance than calibration performance, and even LASCAM15 overestimated streamflow by approximately 20% (median across catchments). This pattern is consistent with previous studies showing that rainfall-runoff models often lose performance when applied to climatic conditions that differ from those used for calibration, particularly when validation periods are drier (e.g., Vaze et al., 2010; Coron et al., 2012, 2014; Saft et al., 2016).

The remaining validation bias should therefore not be interpreted simply as evidence that LASCAM15 is unsuitable for future planning under climate change. The strong calibration performance of LASCAM15 (i.e., outperforming GR4J and SACRAMENTO) confirm that the model is quite flexible in being able to transition between wetter and drier years within the calibration period, as seen by the performance scores which focus on this aspect (see the description of the Split-Trotter objective function in Sect. 4.1.3). However, the validation results suggest more improvement is needed to be able to transition to an independent period that is drier still. As Fowler et al. (2018b) noted, poor model transfer under changing climatic conditions can arise not only from model structural issues but also from other issues such as calibration strategy. Given the emphasis here on LASCAM15 retaining the existing representation of vegetation water use and long-term storage dynamics in the original model, perhaps the calibration strategy should become the focus for further improvement.

Future work should therefore test whether LASCAM15 can be better constrained for drying conditions through revised calibration approaches. Split-Trotter already reduces the dominance of wet years by evaluating model performance separately for each year, but it still calibrates the model using streamflow information alone. This may not be sufficient to constrain the internal processes that control model transfer under drying, particularly vegetation water use and longer-term groundwater storage dynamics (e.g., Burns et al., 2025; Zhang et al., 2026). Multi-objective calibration could therefore be used to incorporate additional constraints from flux-tower evapotranspiration and groundwater-level observations. A key challenge is to develop ways of generalising this information across space, since few flux towers nor groundwater wells exist within gauged catchments in our dataset, while Gravity Recovery and Climate Experiment (GRACE) data present the opposite challenge of being an inherently regional product. In any case, the training of the model on these non-streamflow observations—particularly as they relate to multi-annual behaviour—may improve the ability of models such as LASCAM15 to transfer to future drying conditions.

6.4 Broader implications and recommendations

For complex conceptual models that are already used in applied or operational settings, simplification is not only a technical exercise but also a question of model continuity and usability. Changing the model structure by removing stores or flux pathways can alter model behaviour in ways that are difficult to diagnose and may reduce confidence among existing users. Parameter fixing offers a more conservative pathway: it reduces the number of free calibration dimensions while keeping the original equations and process pathways intact. More broadly, this approach can help identify which parts of a model require catchment-specific calibration and which can be represented using common default values.

This does not mean that parameter fixing is the only useful simplification pathway. Process simplification is an alternative approach and may be appropriate where particular flux pathways or stores are shown to be redundant, weakly identifiable, or unnecessarily complex. For LASCAM, features linked to evapotranspiration and longer-term storage dynamics should be treated cautiously because they are central to the model's value under prolonged dry conditions. Other components, such as the separate infiltration-excess and saturation-excess runoff pathways, could be tested more directly in future work. More exploratory hybrid structures, such as retaining LASCAM's storage and evapotranspiration formulations while testing simpler partitioning schemes, may also help identify which structural features are essential.

Finally, broader application of LASCAM15 requires testing beyond SWWA. The fixed default values and retained calibrated parameters were identified under SWWA hydroclimatic conditions, so their transferability to wetter, more seasonal, or more strongly regulated catchments remains uncertain. Future work should test whether the same simplified configuration is suitable across other Australian regions, or whether region-specific fixed values and parameter sets are needed for national-scale use.

https://doi.org/10.5194/egusphere-2026-4407
Preprint. Discussion started: 12 August 2026

7 Conclusions

This study developed a simplified version of LASCAM, namely LASCAM15, to reduce calibration burden while retaining the model structure that makes it useful for representing catchment response under prolonged dry conditions. The simplification used the latest version of LASCAM (LASCAM22) as the starting point, then applied sensitivity analysis, parameter default-value testing, and stepwise parameter-fixing calibration to identify a more parsimonious configuration. This approach simplified the calibration problem while preserving the main LASCAM stores and flux pathways.

LASCAM15 retains 15 calibrated parameters and fixes seven lower-sensitivity parameters using default values that were shown to work well across catchments. In this way, LASCAM15 reduces unnecessary degrees of freedom while keeping flexibility in the parts of the model where catchment-specific behaviour remains important. The stepwise parameter-fixing calibration supported this configuration as the best balance between dimensionality reduction and performance retention.

The split-sample test showed that LASCAM15 retained most of the calibration strength of LASCAM22 and outperformed GR4J and Sacramento in both calibration and validation. Its stronger validation performance than LASCAM22 further showed that the reduced configuration remained robust under independent evaluation conditions and may indicate over parameterisation in the original model. Overall, LASCAM15 provides a more parsimonious, computationally efficient, and practical version of LASCAM for catchment modelling applications under a drying climate.

Appendix A

Appendix A summarises the relationship between the 28-parameter eWater Source version of LASCAM, referred to as LASCAM28, and the 22-parameter formulation used in this study, referred to as LASCAM22. Both versions were pre-existing to this study, and have the same overall structure but have differing degrees of complexity. In addition to rainfall and potential evapotranspiration as climate inputs, LASCAM28 uses LAI and the proportion of impervious area, to better represent land-use change and urbanisation. The definitions, feasible ranges, and units of the LASCAM28 parameters are provided in Table A1, which mirrors Table 1 for LASCAM22. The key differences between LASCAM28 and LASCAM22 are summarised in Table A2.

https://doi.org/10.5194/egusphere-2026-4407
Preprint. Discussion started: 12 August 2026

Table A1. The definition, feasible range and units for each parameter in LASCAM28.

Parameters	Symbol	Definition	Units	Min	Max
amn	A_{min}	A store reference minimum	mm/day	0	500
amx	A_{max}	A store reference maximum	mm/day	80	1000
bmx	B_{max}	B store reference maximum	mm/day	500	2500
fmx	F_{max}	F store reference maximum	mm/day	200	900
fs0	f_{s0}	Surface infiltration parameter	-	0.001	200
dfs	f_{s1}	Surface infiltration parameter	-	0.001	200
td	t_d	F store recharge parameter	-	1	1500
alphaa	α_a	A store discharge parameter	-	0.001	10
alphab	α_b	B store discharge parameter	-	0.001	10
alphac	α_c	Surface saturation parameter	-	0.0001	10
alphaf	α_f	Subsurface infiltration parameter	-	0.001	10
alphag	α_g	Throughfall parameter	-	-0.2	0.2
alphass	α_{ss}	Subsurface saturation parameter	-	0.1	11
betaa	β_a	A store discharge parameter	-	0.01	10000
betab	β_b	B store discharge parameter	-	0.00001	10
betac	β_c	Surface saturation parameter	-	0	5
betaf	β_f	Subsurface infiltration parameter	-	0.001	10
betag	β_g	Throughfall parameter	-	0	0.2
betass	β_{ss}	Subsurface saturation parameter	-	0	5
gammaa	γ_a	A store evaporation parameter	-	0.001	10
gammab	γ_b	B store evaporation parameter	-	0.1	1
gammaf	γ_f	F store evaporation parameter	-	0.1	0.7
deltab	δ_b	B store evaporation parameter	-	0.1	5
deltaf	δ_f	F store evaporation parameter	-	0.3	1
dmu1	$d\mu_1$	upslope perching parameter	-	0	2
dmu2	$d\mu_2$	upslope perching parameter	-	100	2500
dmu3	$d\mu_3$	upslope perching parameter	-	0.1	2
anrain	anrain	upslope perching parameter	-	300	3000

555

https://doi.org/10.5194/egusphere-2026-4407
Preprint. Discussion started: 12 August 2026

Table A2. Key differences between LASCAM28 and LASCAM22.

Model component	LASCAM28 representation	LASCAM22 representation
Upslope perching	*dmu1*, *dmu2*, *dmu3*, *anrain*	Consolidated into *mu*
Surface saturation	*betac*	Fixed at 1
Subsurface saturation	*betass*	Fixed at 1
Surface infiltration / LAI dependence	*fs0*, *dfs,* with LAI dependence	Simplified to *fs*, with LAI fixed at 1
Impervious area	*Imperv*	Set to 0 / excluded from the equations used here

Appendix B

Appendix B provides the equations for LASCAM22, the formulation used as the starting point for the simplification framework in this study. It is run at a daily timestep using precipitation P_t and potential evapotranspiration $E_{p,t}$ as inputs.

At the beginning of each timestep, throughfall is calculated as:

$$P_{g,t} = \max(\min(\alpha_g + P_t(1-\beta_g), P_t), 0) \tag{B1}$$

and canopy/interception loss is:

$$E_{g,t} = P_t - P_{g,t} \tag{B2}$$

Fractional storage values are calculated as:

$$S_{Apr,t} = \max\left(\frac{S_{A,t}-A_{min}}{A_{max}-A_{min}}, 0\right) \tag{B3}$$

$$S_{Bpr,t} = \max\left(\min\left(\frac{S_{B,t}}{B_{max}}, 1\right), 0\right) \tag{B4}$$

$$S_{Fpr,t} = \max\left(\frac{S_{F,t}}{F_{max}}, 0.0001\right) \tag{B5}$$

where $S_{A,t}$, $S_{B,t}$, and $S_{F,t}$ are storage values of A store, B store and F store at current timestep.

A-store discharge is then calculated as:

$$q_{a,t} = \begin{cases} \min(\beta_a {S_{Apr,t}}^{\alpha_a}, \mu), & S_{A,t} > A_{min} \\ 0, & S_{A,t} \leq A_{min} \end{cases} \tag{B6}$$

where μ is the upslope perching parameter.

https://doi.org/10.5194/egusphere-2026-4407
Preprint. Discussion started: 12 August 2026

The subsurface saturated-area fractions $\varphi_{ss,t}$ and surface saturated-area fractions $\varphi_{c,t}$ are calculated as:

$$\varphi_{ss,t} = \begin{cases} \min(\alpha_{ss} S_{Apr,t}, \mu), & S_{A,t} > A_{min} \\ 0, & S_{A,t} \leq A_{min} \end{cases} \tag{B7}$$

$$\varphi_{c,t} = \begin{cases} \min(\alpha_c S_{Apr,t}, \varphi_{ss,t}), & S_{A,t} > A_{min} \\ 0, & S_{A,t} \leq A_{min} \end{cases} \tag{B8}$$

Surface saturation-excess runoff is:

$$q_{se,t} = \varphi_{c,t} P_{g,t} \tag{B9}$$

Surface infiltration-excess runoff is:

$$q_{ie,t} = \begin{cases} (\mu - \varphi_{c,t}) P_{g,t} \left(1 - \frac{f_s}{P_{g,t}}\right)^2, & P_{g,t} > f_s \\ 0, & P_{g,t} \leq f_s \end{cases} \tag{B10}$$

where f_s is the surface infiltration parameter.

The subsurface infiltration capacity is calculated as:

$$f_{ss,t} = \frac{\alpha_f (1 - S_{Bpr,t})}{{S_{Fpr,t}}^{\beta_f}} \tag{B11}$$

The infiltration available to subsurface pathway is:

$$I_t = \begin{cases} P_{g,t} - \frac{q_{ie,t}}{\mu - \varphi_{c,t}}, & \varphi_{c,t} < \mu \\ 0, & \varphi_{c,t} \geq \mu \end{cases} \tag{B12}$$

Subsurface saturation-excess runoff is:

$$q_{sse,t} = \begin{cases} (\varphi_{ss,t} - \varphi_{c,t}) I_t, & \varphi_{c,t} < \mu \\ 0, & \varphi_{c,t} \geq \mu \end{cases} \tag{B13}$$

Subsurface infiltration-excess runoff is:

$$q_{sie,t} = \begin{cases} \max\left((\mu - \varphi_{ss,t}) \left(I_t - \frac{f_{ss,t}}{1 - \varphi_{ss,t}}\right), 0\right), & \varphi_{c,t} < \mu \text{ and } \varphi_{ss,t} < 1 \\ 0, & otherwise \end{cases} \tag{B14}$$

Total subsurface runoff is:

$$q_{ss,t} = q_{sse,t} + q_{sie,t} \tag{B15}$$

https://doi.org/10.5194/egusphere-2026-4407
Preprint. Discussion started: 12 August 2026

Subsurface infiltration into the F store is:

$$f_{a,t} = \max(P_{g,t} - q_{se,t} - q_{ie,t} - q_{ss,t}, 0) \tag{B16}$$

Recharge from A store to B store is:

$$r_{2,t} = \min(\varphi_{ss,t} f_{ss,t}, min(10, \max(S_{A,t}, 0))) \tag{B17}$$

Evaporation from A store is calculated as:

$$E^*_{a,t} = \begin{cases} 0, \; S_{A,t} < 0 \\ E_{p,t}\gamma_a \frac{\sqrt{A_{min}S_{A,t}}}{A_{max}}, \; 0 < S_{A,t} < A_{min} \\ E_{p,t}\frac{S_{A,t}+A_{min}(\gamma_a - 1)}{A_{max}}, \; S_{A,t} \geq A_{min} \end{cases} \tag{B18}$$

with the final A-store evaporation limited by potential evapotranspiration:

$$E_{a,t} = \min(E^*_{a,t}, E_{p,t}) \tag{B19}$$

Recharge from F store to B store is:

$$r_{1,t} = \begin{cases} \frac{S_{F,t}}{t_d}, \; S_{F,t} \geq 0 \\ 0, \; S_{F,t} < 0 \end{cases} \tag{B20}$$

Potential F-store evaporation before storage constraints is:

$$E^*_{f,t} = \left(E_{p,t} - E_{a,t}\right) * \max(1 - \gamma_f {S_{Fpr,t}}^{-\delta_f}, 0) \tag{B21}$$

and actual F-store evaporation is:

$$E_{f,t} = \begin{cases} \max(\min\left(E^*_{f,t}, E_{p,t} - E_{a,t}, S_{F,t} + f_{a,t} - r_{1,t}\right), 0), \; S_{F,t} \geq 0 \\ 0, \; S_{F,t} < 0 \end{cases} \tag{B22}$$

B-store discharge is:

$$q_{b,t} = \begin{cases} \mu\beta_b(\exp\left(\alpha_b S_{Bpr,t}\right) - 1), \; S_{B,t} \geq 0 \\ 0, \; S_{B,t} < 0 \end{cases} \tag{B23}$$

The remaining potential evapotranspiration after A- and F-store evaporation is:

$$E_{p\_left,t} = E_{p,t} - E_{a,t} - E_{f,t} \tag{B24}$$

Evaporation from B store is:

$$E_{b,t} = \begin{cases} \max(\min\left(\gamma_b * E_{p\_left,t} * {S_{Bpr,t}}^{\delta_b}, E_{p\_left,t}\right), 0), \; S_{B,t} \geq 0 \\ 0, \; S_{B,t} < 0 \end{cases} \tag{B25}$$

https://doi.org/10.5194/egusphere-2026-4407
Preprint. Discussion started: 12 August 2026

The three stores are updated as:

$$S_{A,t+1} = S_{A,t} + q_{ss,t} + q_{b,t} - E_{a,t} - r_{2,t} - q_{a,t} \quad \text{(B26)}$$

$$S_{B,t+1} = S_{B,t} + r_{2,t} - q_{b,t} - E_{b,t} + r_{1,t} \quad \text{(B27)}$$

$$S_{F,t+1} = S_{F,t} + f_{a,t} - r_{1,t} - E_{f,t} \quad \text{(B28)}$$

Finally, simulated streamflow is calculated as:

$$Q_{sim,t} = q_{se,t} + q_{ie,t} + q_{a,t} \quad \text{(B29)}$$

Code availability

The exact version of the Python code, processing scripts, configuration files, and other materials used to produce the results presented in this study is available at GitHub, linked to Zenodo at https://doi.org/10.5281/zenodo.21465140 (Zhang, 2026). The GR4J and Sacramento models used in this study were reimplemented in Python based on their implementations in the hydromad R package (Andrews et al., 2021), enabling consistent implementation and comparison across all models.

Data availability

Daily climate inputs for the selected catchments were obtained from the SILO climate database (https://www.longpaddock.qld.gov.au/silo/point-data). Daily streamflow data were obtained mainly from the CAMELS-AUS v2 database (Fowler et al., 2025), supplemented by records from the DWER Water Information Reporting database (http://wir.water.wa.gov.au) for stations not included in CAMELS-AUS v2.

Author contributions

ZZ: Conceptualisation, formal analysis, visualization, investigation, methodology, writing – original draft, review and editing.

KF: Conceptualisation, methodology, supervision, writing – review and editing

MT: Conceptualisation, methodology, supervision, writing – review and editing

JH: Conceptualisation, methodology, supervision, writing – review and editing

Competing interests

The authors declare that they have no conflict of interest.

https://doi.org/10.5194/egusphere-2026-4407
Preprint. Discussion started: 12 August 2026

Financial support

This research has been supported by funding from the Western Australian Department of Water and Environmental Regulation as part of the Climate Adaptation Strategy program: *Understanding how climate change impacts Water Resources in Western Australia - Communication and Research Initiative*.

References

Alvarez-Garreton, C., Boisier, J. P., Garreaud, R., Seibert, J., and Vis, M.: Progressive water deficits during multiyear droughts in basins with long hydrological memory in Chile, Hydrology and Earth System Sciences, 25, 429–446, https://doi.org/10.5194/hess-25-429-2021, 2021.

Andrews, F., Guillaume, J., Vervoort, W., and Buzacott, A.: hydromad: Hydrological Model Assessment and Development, 2021.

Arsenault, R., Poulin, A., Pardalos, P. M., and Brissette, F.: Comparison of Stochastic Optimization Algorithms in Hydrological Model Calibration, Journal of Hydrologic Engineering, 19, 1374–1384, https://doi.org/10.1061/(asce)he.1943-5584.0000938, 2014.

Arsenault, R., Brissette, F., and Martel, J.-L.: The hazards of split-sample validation in hydrological model calibration, Journal of Hydrology, 566, 346–362, https://doi.org/10.1016/j.jhydrol.2018.09.027, 2018.

Avanzi, F., Rungee, J., Maurer, T., Bales, R., Ma, Q., Glaser, S., and Conklin, M.: Climate elasticity of evapotranspiration shifts the water balance of Mediterranean climates during multi-year droughts, Hydrology and Earth System Sciences, 24, 4317–4337, https://doi.org/10.5194/hess-24-4317-2020, 2020.

Beven, K.: A manifesto for the equifinality thesis, Journal of Hydrology, 320, 18–36, https://doi.org/10.1016/j.jhydrol.2005.07.007, 2006.

Burns, G., Fowler, K., Peel, M., and Stephens, C.: A systematic evaluation of 15 actual evapotranspiration formulations within conceptual hydrological models, EGUsphere [preprint], 2025, 1–30, https://doi.org/10.5194/egusphere-2025-3122, 2025.

Campion, N., Fowler, K., Turner, M., and Hall, J.: Hydrological non-stationarity in south-west western australia, Zenodo [data set], https://doi.org/10.5281/zenodo.15836564, 2024.

Campion, N., Fowler, K., Turner, M., and Hall, J.: Comparing drivers of hydrological shifts across regions: the case of southern Australia, EGUsphere [preprint], 2026, 1–35, https://doi.org/10.5194/egusphere-2026-378, 2026.

Cook, B. I., Mankin, J. S., and Anchukaitis, K. J.: Climate Change and Drought: from past to Future, Current Climate Change Reports, 4, 164–179, https://doi.org/10.1007/s40641-018-0093-2, 2018.

Coron, L., Andréassian, V., Perrin, C., Lerat, J., Vaze, J., Bourqui, M., and Hendrickx, F.: Crash testing hydrological models in contrasted climate conditions: An experiment on 216 Australian catchments, Water Resources Research, 48, https://doi.org/10.1029/2011wr011721, 2012.

Coron, L., Andréassian, V., Perrin, C., Bourqui, M., and Hendrickx, F.: On the lack of robustness of hydrologic models regarding water balance simulation: a diagnostic approach applied to three models of increasing complexity on 20 mountainous catchments, Hydrology and Earth System Sciences, 18, 727–746, https://doi.org/10.5194/hess-18-727-2014, 2014.

Fowler, K., Peel, M., Western, A., and Zhang, L.: Improved Rainfall-Runoff Calibration for Drying Climate: Choice of Objective Function, Water Resources Research, 54, 3392–3408, https://doi.org/10.1029/2017wr022466, 2018a.

Fowler, K., Coxon, G., Freer, J., Peel, M. C., Wagener, T., Western, A. W., Woods, R., and Zhang, L.: Simulating Runoff Under Changing Climatic Conditions: A Framework for Model Improvement, Water Resources Research, 54, 9812–9832, https://doi.org/10.1029/2018wr023989, 2018b.

Fowler, K., Knoben, W., Peel, M., Peterson, T., Ryu, D., Saft, M., Seo, K., and Western, A.: Many Commonly Used Rainfall-Runoff Models Lack Long, Slow Dynamics: Implications for Runoff Projections, Water Resources Research, 56, https://doi.org/10.1029/2019wr025286, 2020.

Fowler, K., Peel, M., Saft, M., Peterson, T. J., Western, A., Band, L., Petheram, C., Dharmadi, S., Tan, K. S., Zhang, L., Lane, P., Kiem, A., Marshall, L., Griebel, A., Medlyn, B. E., Ryu, D., Bonotto, G., Wasko, C., Ukkola, A., and Stephens, C.: Explaining changes in rainfall–runoff relationships during and after Australia's Millennium Drought: a community perspective, Hydrology and Earth System Sciences, 26, 6073–6120, https://doi.org/10.5194/hess-26-6073-2022, 2022.

Fowler, K. J. A., Zhang, Z., and Hou, X.: CAMELS-AUS v2: updated hydrometeorological time series and landscape attributes for an enlarged set of catchments in Australia, Earth System Science Data, 17, 4079–4095, https://doi.org/10.5194/essd-17-4079-2025, 2025.

George, R. J., Bell, R.-A., McCaw, W. L., and Raper, G. P.: A Multidecadal Analysis of Groundwater Level and Streamflow Decline in Southern Forest Catchments, Western Australia, Journal of the Royal Society of Western Australia, 108, https://doi.org/10.70880/001c.144793, 2025.

Gilles, Arsenault, R., and Brissette, F.: Comparison of climate datasets for lumped hydrological modeling over the continental United States, Journal of Hydrology, 537, 334–345, https://doi.org/10.1016/j.jhydrol.2016.03.063, 2016.

Gupta, H. V., Kling, H., Yilmaz, K. K., and Martinez, G. F.: Decomposition of the mean squared error and NSE performance criteria: Implications for improving hydrological modelling, Journal of Hydrology, 377, 80–91, https://doi.org/10.1016/j.jhydrol.2009.08.003, 2009.

Hughes, J. D., Petrone, K. C., and Silberstein, R. P.: Drought, groundwater storage and stream flow decline in southwestern Australia, Geophysical Research Letters, 39, n/a-n/a, https://doi.org/10.1029/2011gl050797, 2012.

Jakeman, A. J. and Hornberger, G. M.: How much complexity is warranted in a rainfall-runoff model?, Water Resources Research, 29, 2637–2649, https://doi.org/10.1029/93wr00877, 1993.

KLEMEŠ, V.: Operational testing of hydrological simulation models, Hydrological Sciences Journal, 31, 13–24, https://doi.org/10.1080/02626668609491024, 1986.

https://doi.org/10.5194/egusphere-2026-4407
Preprint. Discussion started: 12 August 2026

Knoben, W. J. M., Freer, J. E., Fowler, K. J. A., Peel, M. C., and Woods, R. A.: Modular Assessment of Rainfall–Runoff Models Toolbox (MARRMoT) v1.2: an open-source, extendable framework providing implementations of 46 conceptual hydrologic models as continuous state-space formulations, Geoscientific Model Development, 12, 2463–2480, https://doi.org/10.5194/gmd-12-2463-2019, 2019.

Laurène J. E. Bouaziz, Fabrizio Fenicia, Guillaume Thirel, Tanja de Boer-Euser, Joost Buitink, Brauer, C. C., Jan De Niel, Dewals, B. J., Gilles Drogue, Grelier, B., Melsen, L. A., Moustakas, S., Jiri Nossent, Pereira, F., Sprokkereef, E., Stam, J., Weerts, A. H., Willems, P., Hubert, and Hrachowitz, M.: Behind the scenes of streamflow model performance, Hydrology and earth system sciences, 25, 1069–1095, https://doi.org/10.5194/hess-25-1069-2021, 2021.

Lehner, F., Coats, S., Stocker, T. F., Pendergrass, A. G., Sanderson, B. M., Raible, C. C., and Smerdon, J. E.: Projected drought risk in 1.5°C and 2°C warmer climates, Geophysical Research Letters, 44, 7419–7428, https://doi.org/10.1002/2017gl074117, 2017.

Massari, C., Avanzi, F., Bruno, G., Gabellani, S., Penna, D., and Luca Brocca: Evaporation enhancement drives the European water-budget deficit during multi-year droughts, Hydrology and Earth System Sciences, 26, 1527–1543, https://doi.org/10.5194/hess-26-1527-2022, 2022.

Mathevet, T., Michel, C., Andréassian, V., and Perrin, C.: Large Sample Basin Experiments for Hydrological Model Parameterization: Results of the Model Parameter Experiment-MOPEX. A bounded version of the Nash-Sutcliffe criterion for better model assessment on large sets of basins, IAHS Publ, 307, 2006.

Perrin, C., Michel, C., and Andréassian, V.: Does a large number of parameters enhance model performance? Comparative assessment of common catchment model structures on 429 catchments, Journal of Hydrology, 242, 275–301, https://doi.org/10.1016/s0022-1694(00)00393-0, 2001.

Peterson, T. J., Saft, M., Peel, M. C., and John, A.: Watersheds may not recover from drought, Science, 372, 745–749, https://doi.org/10.1126/science.abd5085, 2021.

Saft, M., Peel, M. C., Western, A. W., Perraud, J.-M., and Zhang, L.: Bias in streamflow projections due to climate-induced shifts in catchment response, Geophysical Research Letters, 43, 1574–1581, https://doi.org/10.1002/2015gl067326, 2016.

Saltelli, A., Annoni, P., Azzini, I., Campolongo, F., Ratto, M., and Tarantola, S.: Variance based sensitivity analysis of model output. Design and estimator for the total sensitivity index, Computer Physics Communications, 181, 259–270, https://doi.org/10.1016/j.cpc.2009.09.018, 2010.

Sivapalan, M., Ruprecht, J. K., and Viney, N. R.: Water and salt balance modelling to predict the effects of land-use changes in forested catchments. 1. Small catchment water balance model, Hydrological Processes, 10, 393–411, https://doi.org/10.1002/(sici)1099-1085(199603)10:3%3C393::aid-hyp307%3E3.0.co;2-#, 1996a.

Sivapalan, M., Viney, N. R., and Ruprecht, J. K.: Water and salt balance modelling to predict the effects of land-use changes in forested catchments. 2. coupled model of water and salt balances, Hydrological Processes, 10, 413–428, https://doi.org/10.1002/(sici)1099-1085(199603)10:3%3C413::aid-hyp308%3E3.0.co;2-1, 1996b.

https://doi.org/10.5194/egusphere-2026-4407
Preprint. Discussion started: 12 August 2026

Sivapalan, M., Viney, N. R., and Jeevaraj, C. G.: Water and salt balance modelling to predict the effects of land-use changes in forested catchments. 3. The large catchment model, Hydrological Processes, 10, 429–446, https://doi.org/10.1002/(sici)1099-1085(199603)10:3%3C429::aid-hyp309%3E3.0.co;2-g, 1996c.

Sivapalan, M., Viney, N. R., and Zammit, C.: LASCAM: largescale catchment model, in: Mathematical Models of Large Watershed Hydrology, edited by: Singh, V. P. and Frevert, D. K., Water Resources Publications, 2002.

Trotter, L., Knoben, W. J. M., Fowler, K. J. A., Saft, M., and Peel, M. C.: Modular Assessment of Rainfall–Runoff Models Toolbox (MARRMoT) v2.1: an object-oriented implementation of 47 established hydrological models for improved speed and readability, Geoscientific Model Development, 15, 6359–6369, https://doi.org/10.5194/gmd-15-6359-2022, 2022.

Trotter, L., Saft, M., Peel, M. C., and Fowler, K. J. A.: Symptoms of Performance Degradation During Multi-Annual Drought: A Large-Sample, Multi-Model Study, Water Resources Research, 59, https://doi.org/10.1029/2021wr031845, 2023.

Vaze, J., Post, D. A., Chiew, F. H. S., Perraud, J.-M. ., Viney, N. R., and Teng, J.: Climate non-stationarity – Validity of calibrated rainfall–runoff models for use in climate change studies, Journal of Hydrology, 394, 447–457, https://doi.org/10.1016/j.jhydrol.2010.09.018, 2010.

Viney, N. R. and Sivapalan, M.: A conceptual model of sediment transport: application to the Avon River Basin in Western Australia, Hydrological Processes, 13, 727–743, https://doi.org/10.1002/(sici)1099-1085(19990415)13:5%3C727::aid-hyp776%3E3.0.co;2-d, 1999.

Viney, N. R. and Sivapalan, M.: Modelling catchment processes in the Swan-Avon river basin, Hydrological Processes, 15, 2671–2685, https://doi.org/10.1002/hyp.301, 2001.

Viney, N. R., Sivapalan, M., and Deeley, D.: A conceptual model of nutrient mobilisation and transport applicable at large catchment scales, Journal of Hydrology, 240, 23–44, https://doi.org/10.1016/s0022-1694(00)00320-6, 2000.

Viney, N. R., Perraud, J., Vaze, J., Chiew, F. H. S., Post, D. A., and Yang, A.: The usefulness of bias constraints in model calibration for regionalisation to ungauged catchments , in: 18th World IMACS / MODSIM Congress, Cairns, Australia, 2009.

Welsh, W. D., Vaze, J., Dutta, D., Rassam, D., Rahman, J. M., Jolly, I. D., Wallbrink, P., Podger, G. M., Bethune, M., Hardy, M. J., Teng, J., and Lerat, J.: An integrated modelling framework for regulated river systems, Environmental Modelling & Software, 39, 81–102, https://doi.org/10.1016/j.envsoft.2012.02.022, 2013.

Ye, W., Bates, B. C., Viney, N. R., Murugesu Sivapalan, and Jakeman, A.: Performance of conceptual rainfall-runoff models in low-yielding ephemeral catchments, Water Resources Research, 33, 153–166, https://doi.org/10.1029/96wr02840, 1997.

Zammit, C., Sivapalan, M., Kelsey, P., and Viney, N. R.: Modelling the effects of land-use modifications to control nutrient loads from an agricultural catchment in Western Australia, Ecological Modelling, 187, 60–70, https://doi.org/10.1016/j.ecolmodel.2005.01.024, 2005.

Zhang, Z.: potatohey/LASCAM_simplification: Paper (Version v1.0), Zenodo [code], https://doi.org/10.5281/zenodo.21465140, 2026.

https://doi.org/10.5194/egusphere-2026-4407
Preprint. Discussion started: 12 August 2026

Zhang, Z., Fowler, K., and Peel, M.: Can Conceptual Rainfall-Runoff Models Capture Multi-Annual Storage Dynamics?, Water Resources Research, 62, https://doi.org/10.1029/2025wr042226, 2026.